**Table S1. Strains used in this study**

| Strain | Genotype | Figure |
|---|---|---|
| CHB1566 | *hmnEx801* | 1D |
| CHB1612 | *hmnEx864* | 1E |
| CHB1665 | *hmnEx824* | 1F |
| CHB2721 | *hmnEx1535* | 1G |
| CHB2717 | *hmnEx1533* | 1H |
| CHB2719 | *hmnEx1534* | 1I |
| CHB440 | *dyf-7(ns119)* X; *hmnEx149* | 2B |
| CHB1939 | *hmnEx1105* | 2C |
| CHB436 | *oyIs44* V*; dyf-7(ns119)* X*; hmnEx145* | 2D |
| CHB1530 | *hmnEx799* | 2E |
| CHB1557 | *hmnEx821* | 2F |
| CHB558 | *oyIs44* V*; dyf-7(ns119)* X*; hmnEx216* | 2G |
| N2 | wild type | 3A |
| CHB157 | *dyf-7(ns119)* X | 3B |
| CHB1560 | *dyf-7(ns119)* X; *hmnEx824* | 4B,D |
| CHB2718 | *dyf-7(ns119)* X; *hmnEx1534* | 4C,E |
| CHB1556 | *dyf-7(ns119)* X; *hmnEx864* | 4F |
| CHB2720 | *dyf-7(ns119)* X; *hmnEx1535* | 4G |
| CHB2716 | *dyf-7(ns119)* X; *hmnEx1533* | 4H |
| CHB1743 | *oyIs44* V; *hmnEx954* | 5A |
| CHB1741 | *oyIs44* V; *hmnEx953* | 5A |
| CHB1745 | *oyIs44* V; *hmnEx955* | 5A |
| CHB1739 | *oyIs44* V; *hmnEx952* | 5A |
| CHB1742 | *oyIs44* V; *dyf-7(ns119)* X; *hmnEx954* | 5B |
| CHB1740 | *oyIs44* V; *dyf-7(ns119)* X*; hmnEx953* | 5B |
| CHB1744 | *oyIs44* V; *dyf-7(ns119)* X; *hmnEx955* | 5B |
| CHB1738 | *oyIs44* V; *dyf-7(ns119)* X; *hmnEx952* | 5B |
| PY2417 | *oyIs44* V | 5C |
| CHB99 | *oyIs44* V; *dyf-7(ns117)* X | 5C |
| CHB1211 | *frm-2(hmn162)* III; *oyIs44* V; *dyf-7(ns117)* X | 5C |
| CHB2750 | *frm-2(hmn162)* III; *oyIs44* V; *dyf-7(ns117)* X; *hmnEx1553* | 5C |
| CHB2950 | *hmnEx1667* | 5D, S4A |
| CHB2951 | *hmnEx1668* | 5E, S4B |
| CHB1477 | *hmnEx730* | S1E |
| CHB1343 | *hmnEx660* | S1F |
| CHB1475 | *hmnEx756* | S1G |
| CHB370 | *oyIs44* V; *dyf-7(ns119)* X; *hmnEx97* | S3A |
| CHB443 | *oyIs44* V; *dyf-7(ns119)* X; *hmnEx151* | S3A |
| CHB436 | *oyIs44* V; *dyf-7(ns119)* X; *hmnEx145* | S3A |
| CHB1613 | *hmnEx865* | S3B |
| CHB1615 | *hmnEx867* | S3C |

**Table S2. Transgenes used in this study**

A. Stably integrated transgenes

| **Allele** | **Plasmids** | **Reference** |
|---|---|---|
| *oyIs44* | *odr-1*pro:RFP, *lin-15(+)* | P. Sengupta, unpublished |
| *hmnIs27* | pCW11, pDP#MM051 | this study |

B. Unstable extrachromosomal transgenes

| **Allele** | **Plasmids** |
|---|---|
| *hmnEx97* | pMH285, pRF4 |
| *hmnEx145* | pCW11, pRF4 |
| *hmnEx149* | pCW13, pRF4 |
| *hmnEx151* | pCW12, pRF4 |
| *hmnEx216* | pCW32, pCW33, pRF4 |
| *hmnEx660* | pIL11, pIL12, pRF4 |
| *hmnEx730* | pCW94, pIL34, pMH339 |
| *hmnEx756* | pCW93, pIL23, pMH2 |
| *hmnEx762* | pCW31, pMH28, pRF4 |
| *hmnEx799* | pCW34, pIL1, pRF4 |
| *hmnEx801* | pKM15, pKM16, pMH91, pMH130 |
| *hmnEx821* | pCW32, pCW33, pIL44, pIL45, pRF4 |
| *hmnEx824* | pCW95, pIL34, pIL41 |
| *hmnEx864* | pIL43, pIL34, pMH130 |
| *hmnEx865* | pCW17, pRF4 |
| *hmnEx867* | pIL46, pRF4 |
| *hmnEx952* | pMH434, pMH421, pRF4 |
| *hmnEx953* | pEL5, pMH457, pRF4 |
| *hmnEx954* | pMH419, pMH428, pRF4 |
| *hmnEx955* | pMH424, pMH431, pRF4 |
| *hmnEx1105* | pCW11, pMH406, pRF4 |
| *hmnEx1533* | pMH522, pMH524, pRF4 |
| *hmnEx1534* | pMH523, pMH525, pRF4 |
| *hmnEx1535* | pCY184, pMH510, pRF4 |
| *hmnEx1553* | pMC23, pCY159 |
| *hmnEx1667* | pMC33, pMH406, pRF4 |
| *hmnEx1668* | pMC34, pMH406, pRF4 |

**Table S3. Plasmids used in this study**

| Plasmid | Description | Expression | Notes |
|---|---|---|---|
| pCW11 | *dyf-7*pro:DYF-7(ZP-sfGFP) | | SuperfolderGFP (sfGFP) inserted at position 3 (Supp. Fig. S3A) between ZP domain and CFCS |
| pCW12 | *dyf-7*pro:DYF-7(ZPN-sfGFP-ZPC) | | sfGFP inserted at position 2 (Supp. Fig. S3A) between ZPN and ZPC |
| pCW13 | *dyf-7*pro:DYF-7(ZP-sfGFP)-mCherry | | |
| pCW14 | pAC-DYF-7(sfGFP-ZP) | | sfGFP inserted at position 1 (Supp. Fig. S3A) as in pMH285, for expression in *Drosophila* S2 cells (Fig. 3C) |
| pCW17 | *dyf-7*pro:DYF-7(ZP-sfGFP, ΔCFCS) | | ΔCFCS as in pMH21 (Heiman and Shaham, 2009) |
| pCW32 | *hsp-16.41*pro:DYF-7(ZP-sfGFP) | | *hsp-16.41*pro from pPD49.83 (Andrew Fire); see pCW11 |
| pCW33 | *hsp-16.2*pro:DYF-7(ZP-sfGFP) | | *hsp-16.2*pro from pPD49.78 (Andrew Fire); see pCW11 |
| pCW34 | *pha-4*pro:DYF-7(ZP-sfGFP) | embryo gut | *pha-4*pro from pMH16 (Heiman and Shaham, 2009); see pCW11 |
| pCW93 | *F16F9.3*pro:AJM-1-CFP | amphid sheath | *F16F9.3*pro from pMH2 (Heiman and Shaham, 2009); 2630-bp fragment of AJM-1 cDNA (ATGGATGCA..AATCCACTG) was amplified from wild-type animals, after (Köppen et al., 2001) |
| pCW94 | *odr-1*pro:AJM-1-CFP | amphid AWC and (weakly) AWB | *odr-1*pro after (L'Etoile and Bargmann, 2000); see pCW93 |
| pCW95 | *grl-2*pro:AJM-1-CFP | amphid socket | *grl-2*pro after (Hao et al., 2006a); see pCW93 |
| pCY159 | *unc-122*pro:GFP | coelomocytes | |
| pCY184 | *gcy-5*pro:SAX-7-mApple | amphid ASER | mApple was inserted in the SAX-7S cDNA (gift from Hiroyuki Sasakura and Ikue Mori (Sasakura et al., 2005)) at a position eight codons from its terminus ([...ERPE]-[MVSK...ELYK]-[KGSTSTFV]) |
| pDP#MM051 | *unc-119(+)* | | (Maduro and Pilgrim, 1995) |
| pEL5 | *flp-17*pro:CFP | BAG | *flp-17*pro after (Kim and Li, |

| | | | |
|---|---|---|---|
| | | | 2004) |
| pIL1 | *pha-4*pro:myristyl-mCherry | embryo gut | See pCW34 |
| pIL11 | *grl-2*pro:DLG-1-YFP | amphid socket | 558-bp fragment of DLG-1 cDNA (ATGCATTCG..GTGGTTGAA) was amplified from wild-type animals, after (Lockwood et al., 2008) |
| pIL12 | *F16F9.3*pro:DLG-1-CFP | amphid sheath | See pCW93, pIL11 |
| pIL23 | *F16F9.3*pro:ERM-1-YFP | amphid sheath | See pCW93; ERM-1 cDNA sequence was amplified from yk1728e07 (Yuji Kohara, gift from Verena Göbel) |
| pIL34 | *gcy-5*pro:AJM-1-YFP | amphid ASER | *gcy-5*pro after (Yu et al., 1997); see pCW93 |
| pIL41 | *grl-2*pro:mApple | amphid socket | See pCW95; mApple was a gift from Erin Cram |
| pIL43 | *gcy-5*pro:AJM-1-CFP | amphid ASER | See pIL34, pCW93 |
| pIL44 | *hsp-16.2*pro:myristyl-mCherry | | See pCW33 |
| pIL45 | *hsp-16.41*pro:myristyl-mCherry | | See pCW32 |
| pIL46 | *dyf-7*pro:DYF-7(ΔZP, sfGFP)-mCherry | | In-frame deletion of ZP domain from pCW13 |
| pKM15 | *grl-2*pro:YFP | amphid socket | See pCW95 |
| pKM16 | *F16F9.3*pro:CFP | amphid sheath | See pCW93 |
| pMC23 | *frm-2*pro:*frm-2* genomic region | | 4.9 kb promoter sequence (CACTTGTAG..TATTTTCAG) and 3.0 kb genomic coding sequence (ATGTCCTGG..GACTTTTGA) were amplified from wild-type animals |
| pMC33 | *frm-2*pro:GFP | | See pMC23 |
| pMC34 | *frm-2*pro:FRM-2-GFP | | GFP replacing stop codon of pMC23 |
| pMH2 | *F16F9.3*pro:mCherry | amphid sheath | (Heiman and Shaham, 2009) |
| pMH28 | *dex-1*pro:mCherry | broadly in embryo head | (Heiman and Shaham, 2009) |
| pMH91 | *gcy-7*pro:mCherry | amphid ASEL | *gcy-7*pro after (Yu et al., 1997) |
| pMH130 | *gcy-5*pro:mCherry | amphid ASER | See pIL34 |
| pMH285 | *dyf-7*pro:DYF-7(sfGFP-ZP) | | sfGFP inserted at position 1 (Supp. Fig. S3A) between signal peptide sequence and ZP domain |
| pMH339 | *odr-1*pro:mCherry | amphid AWC and (weakly) | See pCW94 |

| | | | |
|---|---|---|---|
| | | AWB | |
| pMH406 | *dyf-7*pro:myristyl-mCherry | | |
| pMH419 | *dat-1*pro:CFP | CEP | (Gilleland et al., 2015) |
| pMH421 | *flp-8*pro:CFP | URX | (Gilleland et al., 2015) |
| pMH424 | *flp-3*pro:YFP | IL1 | (Gilleland et al., 2015) |
| pMH428 | *ser-2prom3*pro:YFP | OLL | *ser-2prom3* after (Tsalik et al., 2003) |
| pMH431 | *klp-6*pro:CFP | IL2 | *klp-6*pro after (Peden and Barr, 2005) |
| pMH434 | *tol-1*pro:YFP | URY | (Gilleland et al., 2015) |
| pMH457 | *ocr-4*pro:YFP | OLQ | *ocr-4*pro after (Tobin et al., 2002) |
| pMH510 | *gcy-5*pro:SAX-7Δcyt-sfGFP | amphid ASER | SAX-7S cDNA cytoplasmic tail was deleted and replaced with superfolderGFP ([..CRQRG]-[MSKGE..]) |
| pMH522 | *F16F9.3*pro:SAX-7-mApple | amphid sheath | See pCY184 |
| pMH523 | *grl-2*pro:SAX-7-mApple | amphid socket | See pCY184 |
| pMH524 | *F16F9.3*pro:SAX-7Δcyt-sfGFP | amphid sheath | See pMH510 |
| pMH525 | *grl-2*pro:SAX-7Δcyt-sfGFP | amphid socket | See pMH510 |
| pRF4 | *rol-6(su1006)* | | (Mello et al., 1991) |

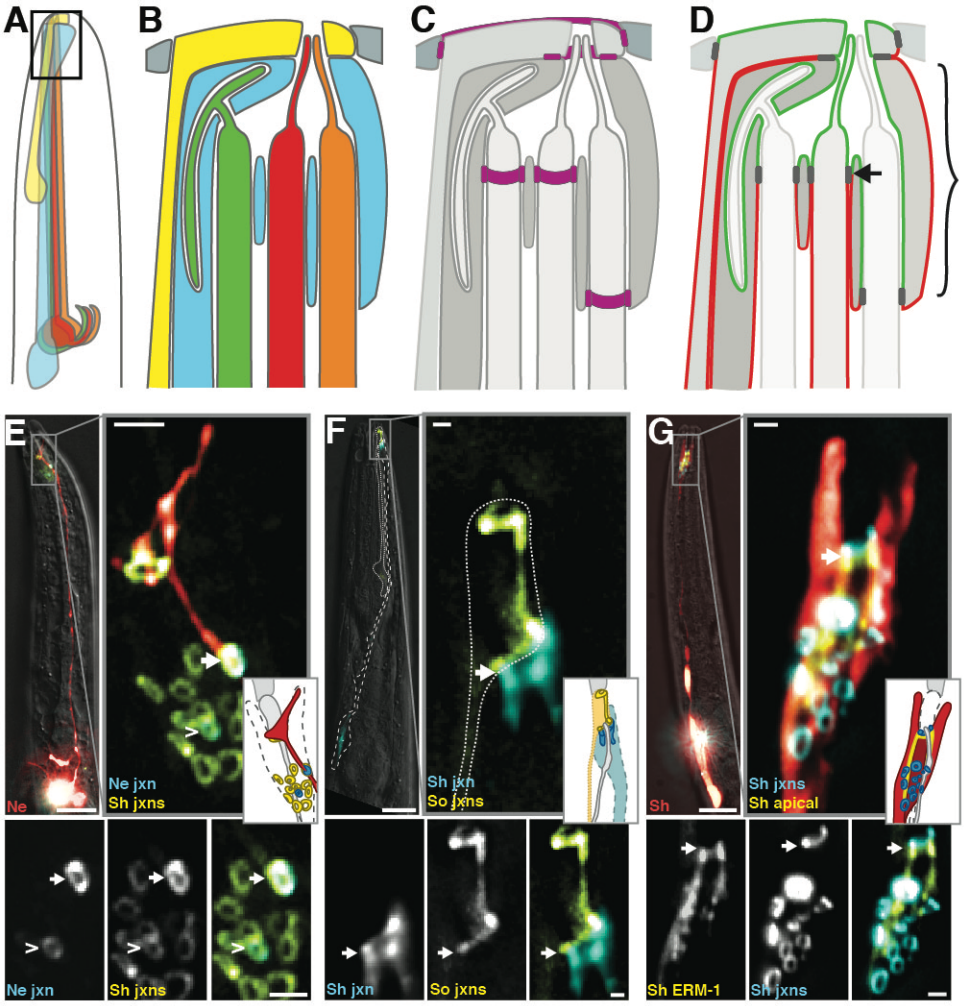


**Figure S1. Markers for tight junctions and apical surfaces**

(A-D) Schematic of amphid showing how different neuron types penetrate the sheath glial cell, based on previous EM reconstructions (Ward et al., 1975; Doroquez et al., 2014). Boxed region in (A) is used to show details of (B) cell morphology, (C) junctions (purple), and (D) apical (green) and basolateral (red) surfaces. The socket glial cell (yellow) forms the outer pore and the sheath glial cell (blue) directly contacts the neurons. The three wing neurons (green; AWA, AWB, AWC) enter the sheath channel and push into the sheath. The eight channel neurons (red and orange; ASE, ADF, ASG,

ASH, ASI, ASJ, ASK, ADL) enter the sheath at stereotyped anterior-posterior positions (compare entry points of red and orange neurons, for example, representing ASE and ASK respectively). The twelfth amphid neuron type, AFD, enters the sheath separately and is enclosed in a private lumen (not shown). The cartoon in (D) is used to illustrate why the apical surface of the sheath may appear more extensive than that of the ASE neurons (compare Fig. 2H with Fig. 2G). ASE forms one of the most anterior junctions with the sheath (D, arrow; see also Fig. 1E), while the apical surface of the sheath extends from the socket to the most posterior neuron entry point (D, bracket). The sheath also contains extensive elaborations of its surface to surround the wing neurons, as well as numerous internal vesicles, that may contribute to this signal. (E-G) Junctions and apical surfaces visualized using other neurons and other markers. (E, F) Overlap of neuron:sheath junctions as in Fig. 1E, except (E) showing AWC (arrow) and AWB (carat) instead of ASE (Ne, AWC neuron (red, *odr-1*pro:RFP, only AWC is shown as AWB expression is dimmer and not visible here); Ne jxn, neuron junctions (blue, *odr-1*pro:AJM-1-CFP); Sh jxns, sheath junctions (yellow, *F16F9.3*pro:AJM-1-YFP)), and (F) using the tight junction marker DLG-1 instead of AJM-1 (Sh jxn, sheath junctions (blue, *F16F9.3*pro:AJM-1-CFP, only sheath:socket junction is shown as sheath:neuron junctions are outside the region of interest); So jxn, socket glial junctions (yellow, *grl-2*pro:DLG-1-YFP)). (G) The apical cytoskelal-associated protein ERM-1 localizes to the outward-facing surface of the sheath (arrow). Sh, sheath glial cell (red, *F16F9.3*pro:mCherry); Sh jxns, sheath junctions (blue, *F16F9.3*pro:AJM-1-CFP); Sh ERM-1 (yellow, *F16F9.3*pro:ERM-1-YFP). Scale bars: 10µm, main panels; 1µm, magnified insets.

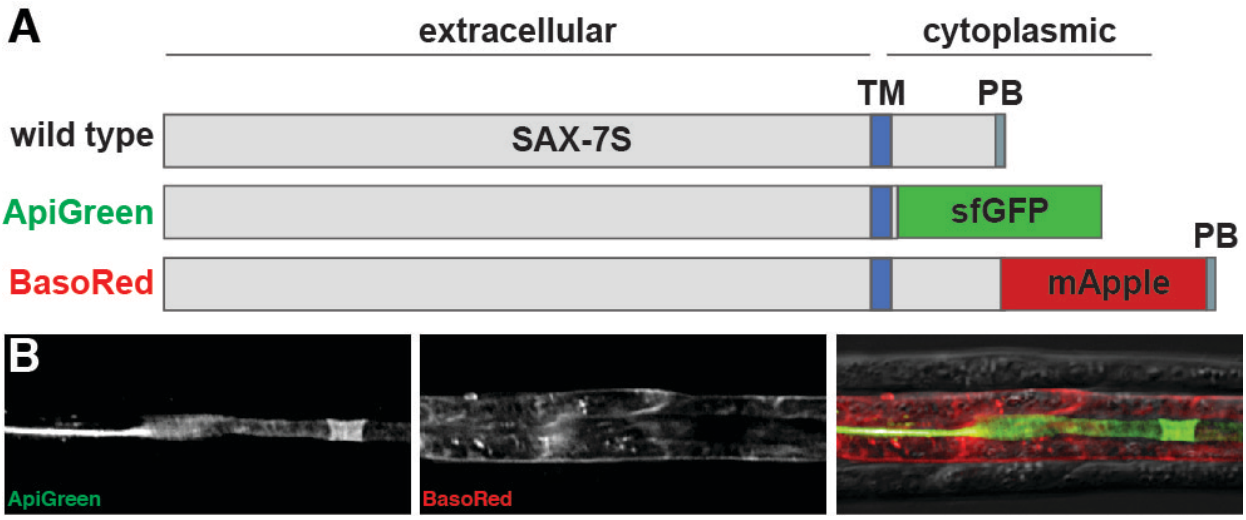


**Figure S2. ApiGreen and BasoRed**

(A) Schematics of the wild-type SAX-7S protein and the ApiGreen and BasoRed constructs that were derived from it. These constructs were based on our observation that full-length SAX-7S localizes to basolateral surfaces, while a construct truncated after the transmembrane segment (TM) is localized to apical surfaces. ApiGreen was created by replacing the SAX-7S cytoplasmic tail with superfolderGFP (pMH510, pMH524, pMH525, Supp. Table S3). BasoRed was created by inserting mApple near the carboxyl-terminus of SAX-7S, before the PDZ-binding motif (PB) (pCY184, pMH522, pMH523, Supp. Table S3). (B) Expression of apical marker ApiGreen and basolateral marker BasoRed in gut, a well-studied model epithelium. The lumen (apical) surface of the gut exhibits localization of ApiGreen and exclusion of BasoRed. A detailed characterization of the sequence motifs responsible for these trafficking patterns, and a survey of how they behave in different cell types at different times across development will be published elsewhere.

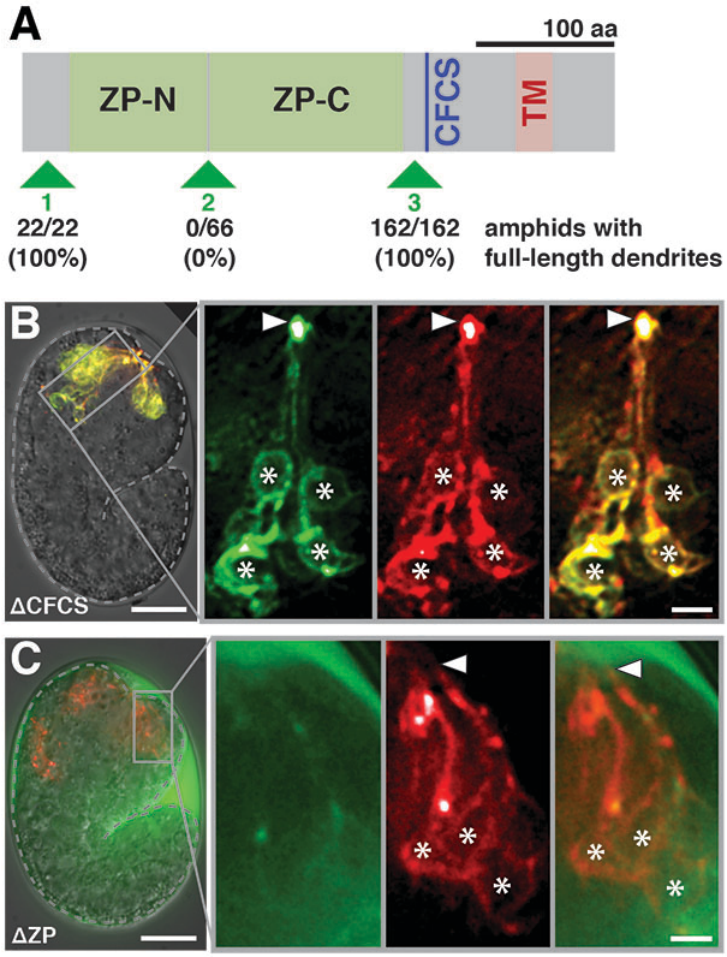


**Figure S3. Localization of DYF-7 *in vivo***

(A) SuperfolderGFP coding sequence was inserted into the DYF-7 cDNA at positions 1, 2, or 3 as indicated (pMH285, pCW12, and pCW11, respectively; Table S1). These constructs were introduced into a strain bearing *dyf-7(ns119)* and an amphid neuron marker (AWC, *odr-1*pro:RFP) and scored for rescue of dendrite extension defects. CFCS, consensus furin cleavage site; TM, transmembrane segment. (B,C) Live, intact embryos expressing sfGFP-DYF-7-mCherry in sensory neurons (*dyf-7*pro) at the time of dendrite extension, as in Fig. 2, but with constructs that are (B) lacking the CFCS (ΔCFCS) or (C) ZP domain (ΔZP). sfGFP, green; mCherry, red; arrowheads, dendrite tips; asterisks, neuron cell bodies. Scale bars: 10µm, main panels; 2µm, magnified insets.

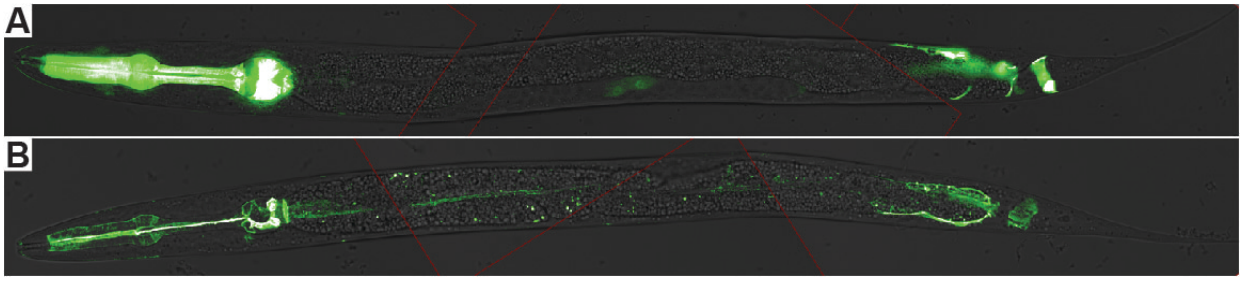


**Figure S4. Expression and localization of FRM-2**

Expression of (A) the transcriptional reporter *frm-2*pro:GFP or (B) the translational fusion *frm-2*pro:FRM-2-GFP in young larvae. Expression is brightest throughout the pharynx, with localization to the apical (luminal) surface. Expression is also observed in cells near the tail, apparently corresponding to the stomato-intestinal and anal depressor muscles which, together with the pharynx, comprise the major non-striated muscle types at this stage. Images are stitched from multiple fields, with borders indicated by red lines.